

Supporting the TECAB Grafting Through CT Based Analysis of Coronary Arteries

Stefan Wesarg

FhG-IGD, Dept. Cognitive Computing & Medical Imaging, Darmstadt, Germany
stefan.wesarg@igd.fraunhofer.de

Abstract. Calcified coronary arteries can cause severe cardiac problems and may provoke an infarction of the heart's wall. An established treatment method is the bypass operation. The usage of a telemanipulation system allows for the execution of that operation as a totally endoscopic coronary artery bypass (TECAB) grafting. This relatively new method narrows the surgeon's view and does not permit the palpation of the vessel in order to detect calcifications (hard plaques).

A planning based on contrast enhanced, cardiac CT data sets can compensate for that problem. This work presents analysis methods for coronary arteries. Hard plaques are detected using a tracking-based vessel segmentation technique. In addition, the vessel's neighborhood is analyzed in order to decide whether it is surrounded by tissue or fat, or if it is freely accessible for the surgeon's instruments. Furthermore, well adapted methods for the visualization of these analysis results are presented.

Keywords: Coronary arteries, vessel segmentation, calcification detection, minimally invasive surgery, cardiac imaging, computed tomography.

1 Introduction

In the developed nations, malfunctions of the cardiovascular system are widespread. Often an obstruction of coronary arteries causes severe risks for the patient's health. The herewith related coronary artery disease (CAD) can hinder the blood-flow towards the areas of the myocardium close to the heart's apex. In the worst case this can provoke an infarction of the heart's wall.

The bypass grafting is an established procedure for the treatment of obstructed coronary arteries. Conventionally, it is executed as open-chest surgery. There, the surgeon can directly look onto the artery and detect hard plaques by palpation of the vessel. New medical devices like 'telemanipulators' change the way that such operations are executed (see fig. 1). They allow for a special form of minimally invasive surgery – the totally endoscopic coronary artery bypass (TECAB) grafting [1, 2].

There, the chest is no longer opened completely, and the intervention can be done on a beating heart. The surgical instruments and an endoscope are inserted into the patient via small ports and controlled by the surgeon from a



Fig. 1. A telemanipulator based system for minimally invasive surgery (*daVinci*, Intuitive Surgical): The surgeon controls the instruments from a console that is providing a stereoscopic view on the operation area (left). The instruments and the endoscope are attached to the arms of the system, and inserted into the patient via ports (right)

console that is providing a stereoscopic view on the operation area. That type of the bypass grafting results in less trauma for the patients, a faster recreation and a much lower infection risk. On the other hand, the TECAB grafting requires more experience of the surgeon due to the limited view during the operation. Finally, only a good planning of the intervention can lead to an optimal result.

An analysis of the coronary artery can compensate for the limitations due to the minimally invasive character of the operation. Considering the fact that a huge amount of time is used for accessing the artery that is often hidden behind fat or muscle tissue, it would be desirable to have this information already prior to the operation. Also, the position of hard plaques should be known before in order to decide where the bypass should be attached to the vessel.

In the past, coronary artery calcium has often been detected based on electron-beam computed tomography (EBCT) data. Several publications describe methods for quantifying the calcium [3, 4], others focus on the reproducibility of the calcium scoring [5]. The reason for the usage of EBCT was the much shorter acquisition time of EBCT compared to conventional computed tomography (CT) of these days.

But the advent of multi-slice computed tomography (MSCT) scanners in combination with a still increased rotation speed now allows for high-quality cardiac imaging based on conventional CT. The simultaneous acquisition of projection data in 16 or more detector rows makes it possible to acquire the whole heart during one single breath-hold [6]. This opens new horizons for the employment of MSCT for cardiac imaging and analysis; especially in the domain of non-invasive coronary angiography [7]. CT based analysis of the coronary arteries is still a relative new technique. Most of the approaches described in the literature are limited to the detection of stenoses and an analysis of 2D image data [8, 9]. To the knowledge of the author there has not been published any work regarding true 3D analysis of coronary arteries based on MSCT coronary angiography yet.

The ‘gold standard’ for the analysis of the coronary artery tree is still conventional angiography. However, this imaging modality is not used for preparing a TECAB grafting. The reason for that is the fact that angiography is an invasive modality that is not suitable for the examination of bypass patients. Furthermore, angiography does not provide any information about the tissue surrounding the coronary artery tree.

There are several publications dealing with the planning of a TECAB grafting using a telemanipulation system. However, the authors mainly focus on the optimization of the port placement for avoiding collisions of the instruments while assuring the reachability of the heart and the coronary artery the surgeon is focusing on [10, 11].

The here presented work introduces methods for localizing calcifications in coronary arteries and inspecting the tissue in their neighborhood aiming on supporting the TECAB grafting in cardiac surgery.

2 Material and Methods

It is desirable to present the image data used for the planning of the intervention in 3D, rather than as conventional 2D slices. However, a 3D view of the image data based on direct volume rendering does neither allow a good perception of coronary arteries and calcium therein, nor the constitution of the surrounding tissue can easily be determined. Therefore, a vessel analysis based on the result of its segmentation is introduced, and well adapted methods for the presentation and exploration of the analysis results are presented.

For the acquisition of our test data a contrast agent has been used to enhance the visibility of the cardiovascular structures. The projection data has been acquired with a multislice CT scanner (SIEMENS *Somatom Sensation 16*) and reconstructed based on the simultaneously recorded ECG data. This resulted in high-quality image data without severe artifacts. The data sets consisted of nearly cubic voxels with a size of about 0.5 mm for each direction.

2.1 Segmentation of Coronary Arteries

We used our own tracking-based vessel segmentation technique that has been developed for the reliable extraction of coronary arteries from high-resolution CT data sets [12]. Vessels, that are containing a contrast agent, are relative homogeneous and show a high contrast with respect to the surrounding tissue. This allows for a detection technique we call the ‘corkscrew algorithm’, and that is truly working in 3D. Thus, a connection between the user defined start and end point following a helical – or corkscrew-shaped – path is searched. It provides in the first step an estimation for the centerline, that is afterwards corrected iteratively by detecting the voxels that belong to the vessel’s border. The algorithm’s output is a set of points defining the centerline and another one representing the border of the artery. For more details see reference [12].

2.2 Hard Plaque Detection

The output of the vessel segmentation presented in the preceding section allows for the subsequent calcification detection. Each computed point of the centerline has a corresponding set of points representing the vessel's border in perpendicular direction to the centerline segment. As a consequence, the diameter of the coronary artery can easily be computed, resulting in a diameter function for the segmented coronary artery.

The employed vessel extraction approach excludes calcifications from the segmentation result. Hence, calcified regions are expected to lower the mean diameter, since the corresponding border points lie 'in front' of them. Based on the generated diameter function and the image data a three-step analysis is performed (see fig. 2):

1. From the diameter function calcification candidates are extracted by selecting those centerline points with a corresponding diameter below a certain threshold. (This could be for instance the mean value of that function.)
2. Afterwards, these candidate points' neighborhoods are searched through whether voxels with high gray values are present. Calcifications are assumed to be 20 % to 30 % brighter than the vessel's lumen that is filled with a contrast agent. Only those candidate points possessing a neighborhood that fulfills that brightness condition are kept.
3. In a last step, the remaining candidate points are analyzed whether they are close to the same calcification. If several candidate points form a group sharing the same calcification, the position laying in the middle between the first and the last point of the group is stored.

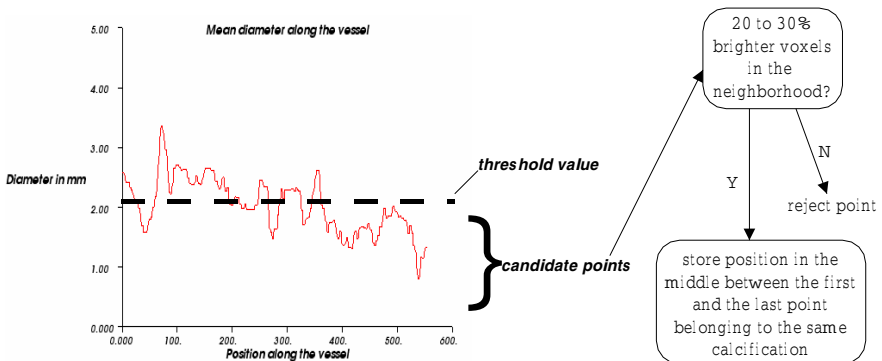


Fig. 2. The analysis for localizing calcifications in coronary arteries: A set of candidate points is selected based on an automatically computed threshold. These points are further analyzed whether bright gray values are in their neighborhood. At the end, the remaining points are decimated again for assuring that only one of them belonging to the same single calcification is stored

The result of that analysis is a set of points with on one hand a position related to a relative low diameter of the coronary artery and on the other hand a neighborhood containing voxels with a high gray value. These two conditions are expected to reliably localize calcifications.

2.3 Inspection of the Artery's Neighborhood

Coronary arteries are often not freely accessible for the surgeon's instruments, since they are surrounded by muscle tissue or fat. The preparation of a TECAB grafting requires the coagulation of that matter in order to isolate the vessel. This procedure is very time-consuming, since it has to be done very prudently in order to not hurting the artery. That process and the TECAB grafting in general could be speed up if there was a possibility for classifying and quantifying the tissue in the vessel's neighborhood.

We propose an analysis method that is based on our vessel segmentation described above. For each set of border points belonging to the same centerline point a set of rays starting from the centerline and passing through the corresponding border points is considered. Along these rays, starting behind the border point, gray value samples from the image data are taken. These values are converted into Hounsfield units (HU) (a task that can easily be done for CT data, since the necessary information is stored in the header of the DICOM¹ data). Based on the obtained HUs the tissue can be roughly classified into air (HU: ≈ -1000), fat (HU: -220 to -20), and muscle tissue (HU: 20 to 50). The length of the rays as well as the sampling rate for the gray value acquisition can be selected by the user.

2.4 Visualization of the Analysis Results

In this section we describe the methods that we have developed for the presentation of the analysis results. They have been designed to be well adapted to the planning of a TECAB grafting. All visualization tasks are done using the freely available toolkit VTK².

The 'natural' way of presenting the generated diameter function is an x - y plot (see left part of fig. 2). For a direct visualization of the diameter function in the volume rendered view, we implemented a filter that creates a tube around the generated centerline. This tube's cross-section dimension varies the same way the diameter function does. In addition, it is colored based on the diameter values. A red color signifies a low diameter, whereas a blue color stands for a large one (see fig. 3).

For visualizing the results of the hard plaque detection multiple cone-shaped pointers are used for indicating the detected calcifications directly in the 3D view. In addition, their positions are given in a list box control. By clicking

¹ The DICOM standard (Digital Imaging and Communications in Medicine) (<http://medical.nema.org/>)

² The Visualization Toolkit by Kitware, Inc. (<http://www.vtk.org>)

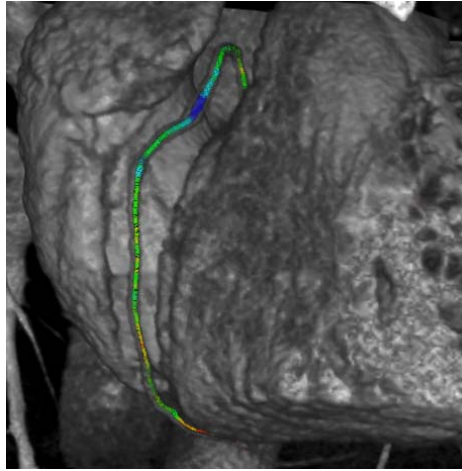


Fig. 3. Visualization of the diameter function directly in the 3D rendered volume of a cardiac MSCT data set: A tube around the computed vessel's centerline is shown. It varies in diameter corresponding to the diameter function. In addition, this variation is color-coded using a linear rainbow-based transition from red to blue. (The artery itself can be perceived as shadow around the generated tube)

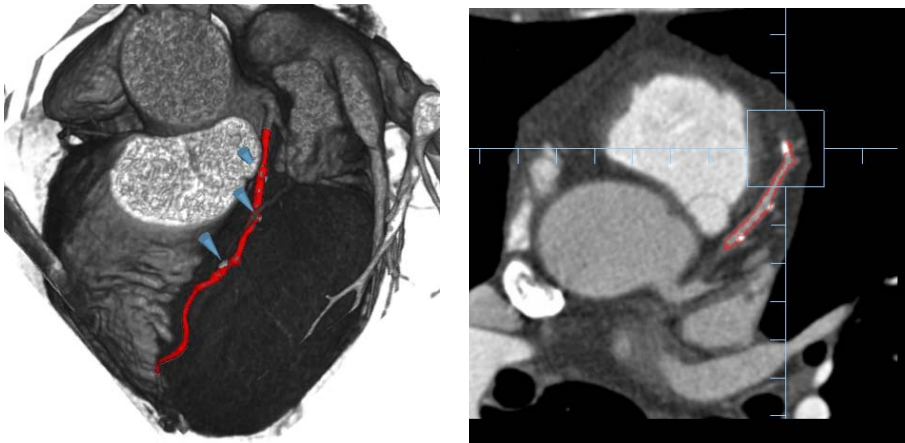


Fig. 4. Detection of multiple hard plaques in a coronary artery: All three calcifications present in the LAD (= left anterior descending) have been detected and are indicated by a pointer (left). Selecting one of them from a list box control adjusts the 2D views and highlights the position of the calcification – axial view shown as example (right)

on one of these entries the corresponding 2D views are shown, highlighting the calcification position (see fig. 4).

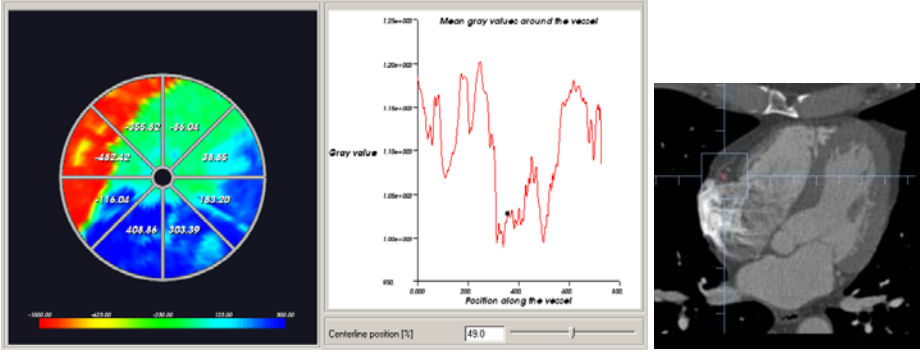


Fig. 5. Visualization of the coronary artery’s neighborhood: A polar plot shows the color coded HUs (red: air, greenish cyan: fat, blueish cyan: muscle, intense blue: contrast filled right atrium and ventricle) for a selected centerline point. The mean gray values of the artery’s neighborhood are shown in an x - y plot (left). Comparison with the corresponding original axial slice shows a strong coincidence with the output of the tissue classification. The small red circle is the outer boundary of the segmented artery. The region’s size shown in the polar plot equals approximately the circle through the square’s corners (right)

A special visualization method for the inspection of the vessel’s neighborhood has been developed. It consists of two outputs. The first one displays the HUs of that neighborhood for each centerline point as color coded values in a polar plot. There, the correct relative dimensions of the vessel’s mean diameter and the selected ray length are used. A slider control allows for navigating along the centerline and inspecting the coronary artery’s neighborhood. An x - y plot displays the mean gray value of the neighborhood for every centerline point.

In addition, the correspondence between this special visualization method and the conventional way of displaying medical image data can easily be verified. For each position along the centerline the 2D views can be aligned according to the x (sagittal), y (coronal), and z (axial) position, and the corresponding point in such a 2D slice is highlighted (see fig. 5). In the 3D view that position is indicated by a small pointer.

3 Results

The proposed analysis techniques have been tested with CT data from 7 patients. For all of them the left anterior descending (LAD), the left circumflex (LCX), and the right coronary artery (RCA) have been segmented using the corkscrew algorithm [12]. The segmentation did not always extract the whole artery due to imaging artifacts that interrupted the continuous run of the vessel. In these cases only that part that has been segmented could be further analyzed.

Table 1. The results for the automatic detection of hard plaques in coronary arteries based on their segmentation: The data sets of seven patients have been used, and in all of them the LAD, the LCX, and the RCA have been inspected

Data set	Hard Plaques	LAD	LCX	RCA
1	Visible	0	0	0
	Detected	0	0	0
2	Visible	3	1	1
	Detected	3	1	1
3	Visible	5	2	5
	Detected	6	2	5
4	Visible	1	0	0
	Detected	1	0	0
5	Visible	3	0	0
	Detected	3	0	0
6	Visible	6	0	1
	Detected	6	0	1
7	Visible	4	0	2
	Detected	5	0	2

The color mapping of the computed artery’s diameter on a tube around the vessel’s centerline allowed for a perception of the change of that parameter along the artery without any difficulty. This way of representing the diameter function is more convenient than providing only its x - y plot.

Table 1 shows the results for the automatic detection of hard plaques. The above introduced automatic technique detected reliably the present calcifications. All of the hard plaques that have been found during a preceding manual inspection of the axial slices have been tracked. Two of them have been indicated twice due to their large size that led the algorithm to an overestimation of the number of calcifications in these cases (data sets 3 and 7). Those segments that did not contain any visible hard plaque have been classified by our technique to be calcification-free, i. e., our tests resulted in a false-positive value of 0.

The method for inspecting the artery’s neighborhood has been tested with the same datasets where the LAD, the LCX, and the RCA have been segmented. There, only a retrospective analysis could be done since the data came from patients whose treatment was already finished. Consequently, we only checked whether the color-coded display of the HUs for the surrounding tissue corresponded to what could be perceived in the conventionally displayed image data. For a run of the artery in axial direction this could simply be done by comparing the colored polar-plot of the analysis window with the axial slice (see fig. 5). For more ‘difficult’ directions of the vessel the other two 2D views as well as the 3D view have been used. In all of the cases this visual evaluation showed a perfect correspondence: Air was displayed red, fat in greenish cyan, and muscle tissue in blueish cyan. In addition, hard plaques and contrast agent filled cavities could easily be perceived since they appeared as intense blue areas.

4 Discussion

The presented, yet preliminary, analysis results using the segmentation output of our tracking-based approach [12] turned out to be robust. The detection of hard plaques delivered in all cases the correct number and positions of the calcifications that have been found by a visual inspection of the image slices. In two cases a single but widespread hard plaque has been detected twice. But, this can not be considered as a serious drawback of our technique. Very important for a clinical use of the automatic hard plaque detection is the false-positive value. Here, the tests resulted in a value of 0 – no false indication of non-existing hard plaque. However, the criteria that the hard plaque detection is based on are of a rather qualitative nature, and an extended, clinical evaluation of our technique is needed (see the end of this section).

The highlighting of the calcifications' positions also in the conventional 2D slices establishes a relationship between the newly introduced technique and the manual inspection of the slices. Thus, radiologists will hopefully accept the automatic technique without reservation, since they can still verify the analysis' output in their habitual way.

Stenoses that may be introduced by calcifications can easily be found when inspecting the vessel's diameter. The proposed method of generating a colored tube that varies in diameter the same way the artery does makes it easy to localize areas of small vessel diameter in the 3D view of the volume. There is no need any longer to mentally map the x - y plot to the image data.

Our method for analyzing the neighborhood of the artery is an innovative approach for providing essential information for the planning of a TECAB grafting. The HU based color coded visualization of the surrounding tissue and air makes it easy for the surgeon to estimate the amount of tissue that has to be removed in order to access the artery.

As a limitation of this work one might consider the fact that the presented methods have been tested only with data from seven patients. We are aware of this, and consequently a clinical study together with our partners from the University Hospital Frankfurt has been started. This study is also aiming on the comparison of our CT based analysis methods with the current 'gold standard' – conventional angiography.

The inspection of the vessel's neighborhood could be done only as a retrospective study of patients whose treatment has already been finished. The aforementioned clinical study will also determine the expected improvements for the TECAB grafting in terms of speeding up the dissection of the artery.

Finally, the here presented methods for visualizing the analysis results are an improvement over existing approaches. But, they are not an optimal solution yet. Therefore, future work will focus on a simulation of the limitations the surgeon is experiencing through the fixed angle view of the used endoscope. In addition, an augmentation of the endoscopic view provided by the telemanipulation system's console with the analysis results would be a possible and useful extension of our proposed approach.

Acknowledgements

We want to thank the clinic for thoracic, cardiological and thorax vasculum surgery of the University Hospital Frankfurt for providing us the CT data sets.

References

1. Loulmet, D., Carpentier, A., d'Attellis, N., Berrebi, A., Cardon, C., Ponzio, O., Aupeple, B., Relland, J.Y.: Endoscopic Coronary Artery Bypass Grafting with the Aid of Robotic Assisted Instruments. *J Thorac Cardiovasc Surg* **118** (1999) 4–10
2. Dogan, S., Aybek, T., Andreßen, E., Byhahn, C., Mierdl, S., Westphal, K., Matheis, G., Moritz, A., Wimmer-Greinecker, G.: Totally Endoscopic Coronary Artery Bypass Grafting on Cardiopulmonary Bypass with Robotically Enhanced Telemanipulation: Report of forty-five Cases. *J Thorac Cardiovasc Surg* **123** (2002) 1125–1131
3. Agatston, A.S., Janowitz, W.R., Hildner, F.J., Zusmer, N.R., Viamonte, M., Detrano, R.: Quantification of Coronary Artery Calcium Using Ultrafast Computed Tomography. *J Am Coll Cardiol* **15** (1990) 827–832
4. Becker, C.R., Knez, A., Jakobs, T.F., Aydemir, S., Becker, A., Schoepf, U.J., Bruening, R., Haberl, R., Reiser, M.F.: Detection and Quantification of Coronary Artery Calcification with Electron-Beam and Conventional CT. *European Radiology* **9** (1999) 620–624
5. Callister, T.Q., Cooil, B., Raya, S.P., Lippolis, N.J., Russo, D.J., Raggi, P.: Coronary Artery Disease: Improved Reproducibility of Calcium Scoring with an Electron-Beam CT Volumetric Method. *Radiology* **208** (1998) 807–814
6. Ohnesorge, B., Flohr, T.: Non-Invasive Cardiac Imaging with Fast Multi-Slice Cardio CT. *electromedica* 68, Siemens AG, Medical Engineering (2000)
7. Traversi, E., Bertoli, G., Barazzoni, G., Baldi, M., Tramarin, R.: Non-Invasive coronary angiography with multislice computed tomography. Technology, methods, preliminary experience and prospects. *Ital Heart J* **5** (2004) 89–98
8. Gerber, T.C., Kuzo, R.S., Karstaedt, N., Lane, G.E., Morin, R.L., Sheedy, P.F., Safford, R.E., Blackshear, J.L., Pietan, J.H.: Current Results and New Developments of Coronary Angiography With Use of Contrast-Enhanced Computed Tomography of the Heart. *Mayo Clin Proc* **77** (2002) 55–71
9. Dewey, M., Schnapauff, D., Laule, M., Lembcke, A., Borges, A.C., Rutsch, W., Hamm, B., Rogalla, P.: Multislice CT Coronary Angiography: Evaluation of an Automatic Vessel Detection Tool. *Fortschr Röntgenstr* **176** (2004) 478–483
10. Cannon, J.W., Stoll, J.A., Selha, S.D., Dupont, P.E., Howe, R.D., Torchiana, D.F.: Port Placement Planning in Robot-Assisted Coronary Artery Bypass. *IEEE Trans. on Robotics and Automation* **19** (2003)
11. Coste-Maniere, E., Adhami, L., Severac-Bastide, R., Lobontiu, A., Salisbury, J.K., Boissonnat, J.D., Swarup, N., Guthart, G., Mousseaux, E., Carpentier, A.: Optimized Port Placement for the Totally Endoscopic Coronary Artery Bypass Grafting using the da Vinci Robotic System. In Rus, D., Singh, S., eds.: *Experimental Robotics VII*. Volume 271 of *Lecture Notes in Control and Information Sciences.*, Springer-Verlag Heidelberg (2001) 199–208
12. Wesarg, S., Firle, E.A.: Segmentation of Vessels: The Corkscrew Algorithm. In Robert L. Galloway, J.E., ed.: *Medical Imaging Symposium 2004*. Volume 5370 of *Proc. of SPIE*. (2004) 1609–1620